Volatile Heterobimetallic Complexes from Pd^{II} and Cu^{II} β-Diketonates: Structure, Magnetic Anisotropy, and Thermal Properties Related to the Chemical Vapor Deposition of Cu–Pd Thin Films

Vladislav V. Krisyuk,*[a] Iraida A. Baidina,[a] Asiya E. Turgambaeva,[a] Vladimir A. Nadolinny,[a] Svetlana G. Kozlova,[a] Ilya V. Korolkov,[a] Thomas Duguet,[b] Constantin Vahlas,[b] and Igor K. Igumenov[a]

A novel approach for preparing volatile heterometallic complexes for use as precursors for the chemical vapor deposition of various materials is reported. New Cu–Pd complexes based on β-diketonate units were prepared, and their structures and compositions were determined. $[PdL_2{*}CuL_2]$ (**1**) and $[PdL_2{*}Cu(tmhd)_2]$ (**2**) (L = 2-methoxy-2,6,6-trimethylheptane-3,5-dionate; tmhd = 2,2,6,6- tetramethylheptane-3,5-dionate) are 1D coordination polymers with alternating metal complexes, which are connected through weak interactions between the Cu atoms and the OCH_3 groups from the ligand of the Pd complexes. The volatility and thermal stability were studied using thermogravimetric and differential thermal analyses and mass spectrometry. Compound **1** vaporizes without decomposition into monometallic complexes. It exhibits magnetic anisotropy, which was revealed from the angular variations in the EPR spectrum of a single crystal. The vapor thermolysis process for **1** was investigated using mass spectrometry, allowing the process to be framed within the temperature range of 200–350 °C. The experimental data, supported by QTAIM calculations of the allowed intermolecular interactions, suggest that **1** likely exists in the gas phase as bimetallic molecules. Compound **1** proved to be suitable as a single-source precursor for the efficient preparation of Cu–Pd alloy films with tunable Cu/Pd ratio. A possible mechanism for the film growth is proposed based on the reported data.

Introduction

Metal–organic complexes are a popular class of molecular materials because they offer variety and flexibility in their molecular design and properties. The construction and characterization of coordination polymers based on these complexes continue to attract attention because they might be useful in catalysis and separations, and in photochemical and electromagnetic applications.[1a–e] Supramolecular structures, assembled from heterometallic complexes as building blocks, possess novel tunable properties because their structures can be easily varied by utilizing the different interactions between the structural units.[1f–k] Heterometallic complexes with various structures and properties are promising precursors for preparing different inorganic materials with multiple components.[2a–e] Metal–organic chemical vapor deposition (MOCVD) is the technique of choice when processing multicomponent films, including thermodynamically metastable phases.[2f–h] Robust MOCVD processes, however, require volatile precursors that are stable under the transport conditions.[2h,i] Among the known heterometallic compounds, complexes with molecules linked through bridging ligands and a combination of two metal atoms are the most common and often explored because numerous combinations of organic ligands that act as bridges are available to bind different metal atoms, forming one structural unit; rational design can produce volatile compounds that are stable.[2i–l]

Heterometallic coordination complexes that can be transported in the gas phase and can be either reassembled in their original form or decomposed on a substrate to produce a desired film are included in our research. Our strategy involves the use of volatile coordination compounds that tend to form polymolecular products in their crystalline form based on the weak coordination bonds between the molecules. For example, we obtained various heterometallic coordination polymers and oligomers through the cocrystallization of Cu^{II}, Pd^{II}, and Pb^{II} β-diketonates.[3] Such heterometallic compounds are formed when transition metal complexes are incorporated be-

[a] *Dr. V. V. Krisyuk, Dr. I. A. Baidina, Dr. A. E. Turgambaeva, Prof. V. A. Nadolinny, Prof. S. G. Kozlova, Dr. I. V. Korolkov, Prof. I. K. Igumenov*
Nikolaev Institute of Inorganic Chemistry SB RAS
3, Acad. Lavrentiev Ave
Novosibirsk 630090 (Russia)
Fax: (+7) 383-3309489
E-mail: kvv@niic.nsc.ru

[b] *Dr. T. Duguet, Dr. C. Vahlas*
Institut Carnot-CIRIMAT, ENSIACET
4, allée Emile Monso, BP-44362
31030 Toulouse Cedex 4 (France)

tween the molecules of the lead complex through the bridging donor atoms of the ligands. Their structural diversity, thermal behavior, and ability to sublimate while retaining their composition and suprastructure largely depend on the composition of the initial monometallic complexes.

In the present work, we describe a complementary approach for organizing the volatile coordination polymers from β-diketonate complexes based on the weak coordination bonds between the molecules. Our approach involves the use of the bridging functionalities of the terminal substituents in the ligand. In particular, the volatile complex CuL_2 (L = 2-methoxy-2,6,6-trimethylheptane-3,5-dionate) forms crystals with 3D-frame packing and weak bridging coordination between the chelated copper atom and the oxygen atom from a methoxy group at the terminal substituents of a ligand of a neighboring molecule.[3f] Thus, by analogy with the previous principle, we can incorporate complexes of another metal that is capable of the same interaction to construct a heterometallic compound. We report that β-diketonate complexes CuL_2 and PdL_2 can form the ordered heterometallic coordination polymer $[PdL_2{*}CuL_2]_n$ (**1**). This approach encouraged us to prepare its structural analogue $[PdL_2{*}Cu(tmhd)_2]_n$ (**2**) (tmhd = 2,2,6,6-tetramethylheptane-3,5-dionate; it does not contain a methoxy group). The aim here is to compare their structure and properties in an attempt to understand basic regularities of formation of heterometallic compounds of this type. The choice of metals is of practical interest because Cu–Pd alloys are often studied as membrane and sensory materials for hydrogen separation.[4] To the best of our knowledge, neither the volatility of heterometallic Cu–Pd compounds nor their use as precursors for the MOCVD of Cu–Pd alloy films have been reported up to now. We recently reported screening results on the MOCVD of Cu–Pd films based on compound **1**, which was chosen by combination of properties as the single-source molecular precursor.[5] It is recalled that Cu-rich Cu–Pd films of tunable elemental and phase composition were obtained at 10 Torr in the temperature range 200 to 350 °C under thermal and/or UV activation of the gas phase. In the present work, we correlate the crystal structure of both compounds **1** and **2** with their magnetic properties, volatility, and gas-phase composition. Moreover, we aim at gaining insights into how the structure of the precursor and the vapor composition correlate with the mechanisms of heterogeneous thermolysis and the elemental composition of the bimetallic films. One of the outcomes of this correlation will be the feasibility of compound **2** to serve as MOCVD precursor.

In that which follows, the crystal structure of the two compounds will be presented first, followed by the QTAIM analysis (quantum theory of atoms in molecules method) of the intermolecular Cu···O interaction in different multimetallic complexes. Then, the EPR spectra and the thermal behavior of the two compounds will be introduced. We will discuss the obtained results in terms of the structure and the thermal and magnetic properties before providing a succinct insight in the elemental composition of the MOCVD processed films from compound **1**. Finally, the conclusions from this work will be summarized before information on the experimental details, in terms of synthesis and characterization of the compounds and of their behavior, is provided.

Results and Discussion

Crystal structure

Compounds **1** and **2** have isotypic crystal structures and the same structural motif; specifically, they are composed of linear coordination polymers of alternating Pd and Cu β-diketonate complexes linked through the additional coordination of methoxy groups from the ligand of the Pd complex with the Cu atoms. In heterometallic compound **1**, the methoxy groups of the Cu complex do not allow for the formation of bridging bonds. Figure 1 shows a chain structure of **1** as an example.

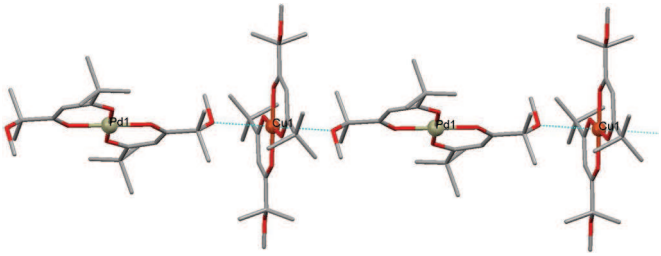

Figure 1. The chain structure of compound **1**. Hydrogen atoms are omitted for clarity. Pd: gray sphere, Cu: red sphere.

The formation of coordination polymers does not significantly modify the structure of molecules of the initial metal complexes, and consequently, no ligand exchange is observed. The bridging Cu–OCH_3 contact distance is 2.916 Å for **1** and 2.951 Å for **2**. As shown in Figure 2, the chains of molecules are packed along the slip planes, forming layers that are orthogonally related. Layers that contain metal atoms of one type can be distinguished in the packing of the molecules, when viewing along the *z*-axis (Figure S1). More detailed study of the structure and properties were carried out for complex **1** because it proved to be more thermally stable than **2**.

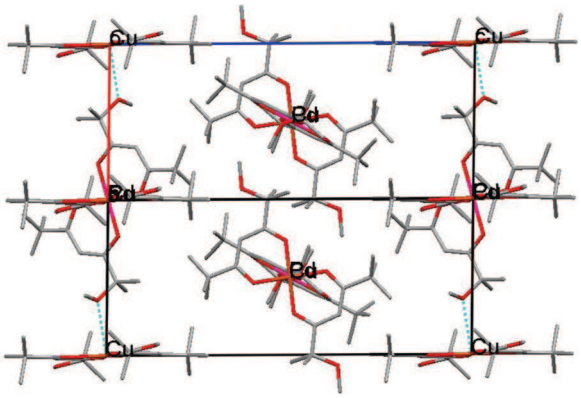

Figure 2. Projection of the crystal packing in **1** along the [−110] direction.

QTAIM analysis of intermolecular Cu···O interaction in the $[CuL_2*PdL_2]$, $[PdL_2*CuL_2*PdL_2]$, and $[CuL_2*PdL_2*CuL_2]$ systems

Figure 3 shows the critical points of the electron density for the $[CuL_2*PdL_2]$ system. The ρs (electron densities) for the intermolecular contacts of the $[CuL_2*PdL_2]$ system are characterized by some Cu···O interactions, which is indicated by the the saddle bonding critical point (*bcp*). Similar points have been found for the following systems: $[CuL_2*PdL_2*CuL_2]$ and $[PdL_2*CuL_2*PdL_2]$. The vibrational spectra were calculated for

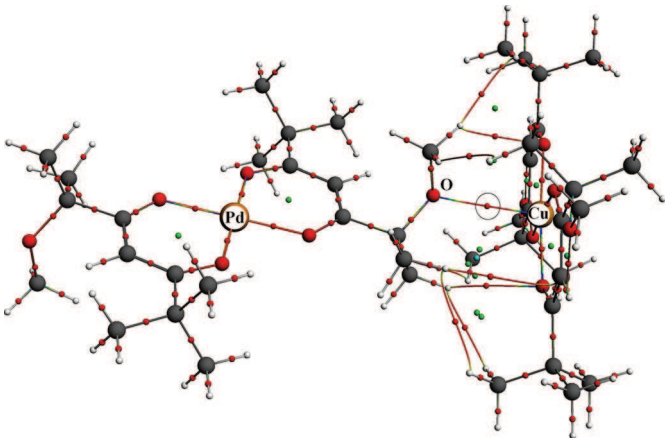

Figure 3. Critical points of electron density for the $[CuL_2*PdL_2]$ system. The *bcp* for the Cu···O contact is marked with a circle.

the optimized structures of $[CuL_2*PdL_2]$, $[PdL_2*CuL_2*PdL_2]$, and $[CuL_2*PdL_2*CuL_2]$; these spectra contain no imaginary frequencies, indicating that these systems are located in the minima (Figure S2). The characteristics of the *bcp*s for the Cu···O contacts are presented in Table 1. According to the QTAIM classifications, these interactions are idealized ones between closed shells and are necessarily weak because $\rho \ll 1$, $\nabla^2\rho > 0$, $E > 0$. For the class of bonds related to the atomic closed shells, the interactions show an increase in the positive value of the total energy density (E) and a decrease in the electron density (ρ) in the *bcp*, weakening the bonds between the atoms. Therefore, the larger the E/ρ ratio is, the lower is the degree of covalent bonding in the intermolecular Cu···O contacts. Therefore, the greatest contribution came from the covalent interactions in the $[CuL_2*PdL_2*CuL_2]$ system, correlating with the calculated length (R) of the Cu···O bond and the binding energy Σ (Table 1).

Table 1. Characteristics of *bcp*s for intermolecular Cu···O contacts in $[CuL_2*PdL_2]$, $[PdL_2*CuL_2*PdL_2]$, and $[CuL_2*PdL_2*CuL_2]$ systems. Electron density (ρ, e Å^{-3}), Laplacian of electron density ($\nabla^2\rho$, e Å^{-5}), density of kinetic energy (G, eVÅ^{-3}), potential energy (U, eV Å^{-3}) and total energy (E, eV Å^{-3}) are presented in atomic units. R is the distance of Cu–O contact (Å) and Σ is the binding energy (eV) of the respective systems.

System	R, Σ	ρ	$\nabla^2\rho$	U	G	E	E/ρ
Initial $[CuL_2*PdL_2]$	2.916, −719.96	0.0756	0.8625	−1.14	1.40	0.26	3.40
Optimized $[CuL_2*PdL_2]$	2.915, −753.31	0.0762	0.8577	−1.14	1.40	0.26	3.13
Optimized $[CuL_2*PdL_2*CuL_2]$	2.847, −1130.03	0.0864	1.0095	−1.38	1.65	0.28	3.19
Optimized $[PdL_2*CuL_2*PdL_2]$	2.988, −1129.64	0.0661	0.0726	−0.94	1.18	0.22	3.33

EPR spectra

The angular variations in the EPR spectra are shown in Figures 4 and 5. An analysis of the angular variation shows that the EPR spectrum is produced by copper(II) ions (Cu^{2+}). The crystal structure of the copper ions presents two magnetic nonequivalent positions, and the spectrum is described by a spin Hamiltonian given in Equation (1)

$$H = g_{xx}\beta H_x S_x + g_{yy}\beta H_y S_y + g_{zz}\beta H_z S_z + A_{xx} S_x I_x + A_{yy} S_y I_y + A_{zz} S_z I_z \quad (1)$$

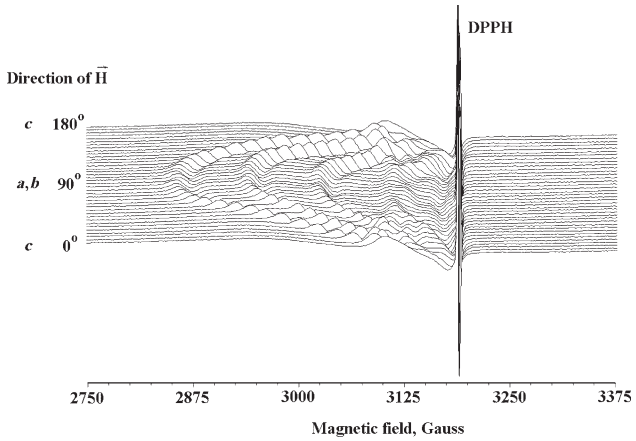

Figure 4. EPR spectra of **1** recorded with an angular variation of the crystal in the {110} plane. DPPH where $g = 2.0036$ is used as a standard g-value.

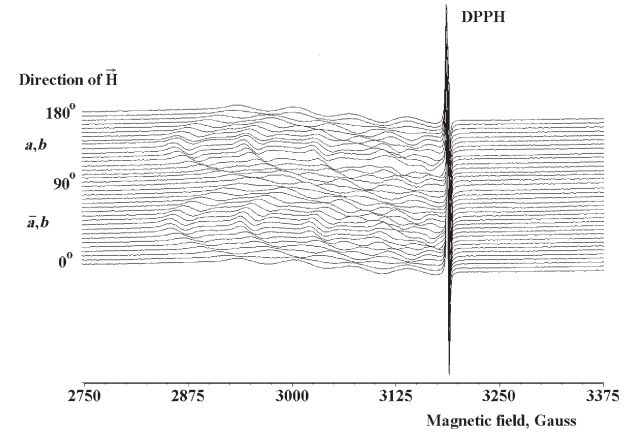

Figure 5. EPR spectra of **1** recorded with an angular variation of a crystal in the {001} plane.

with parameters of $g_{xx}=g_{yy}=2.0365$, $g_{zz}=2.136(8)$, $A_{xx}=A_{yy}=17.8$ Gauss and $A_{zz}=83.6$ Gauss. The EPR spectra of the two copper isotopes ^{63}Cu and ^{65}Cu are unresolved because the width of the individual EPR line is 28 Gauss.

Thermal behavior

The results from the thermogravimetric analysis of the compounds in the condensed phase are presented in Figure 6. Every reported compound exhibits complete mass loss in one step when their condensed phase is heated under atmospheric pressure. The endothermic peak in the density thermal analysis (DTA) curve that corresponds to melting is observed at 176 °C and 183 °C for **1** and **2**, respectively. Figure 7 shows the temperature dependences of the intensities of the selected Cu- and Pd-containing ion peaks derived from the mass spectra recorded while heating the vaporized heterometallic complex **1** and the monometallic complexes CuL_2 and PdL_2. Both Cu- and Pd-containing curves originating from the heterometallic complex are similar, but they differ from the curves from the initial monometallic complexes.

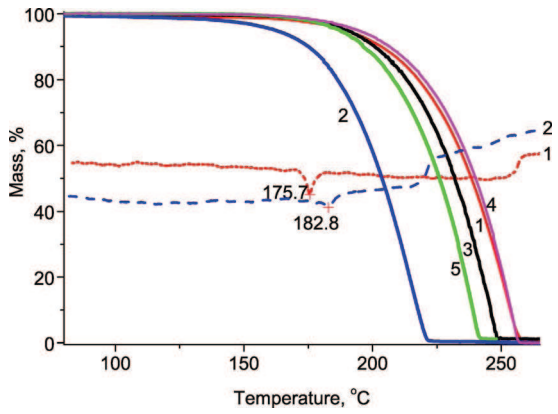

Figure 6. TG (solid)/DTA (dashed) curves for compounds **1** and **2**, PdL_2 (labeled 3), CuL_2 (4), and $Cu(tmhd)_2$ (5).

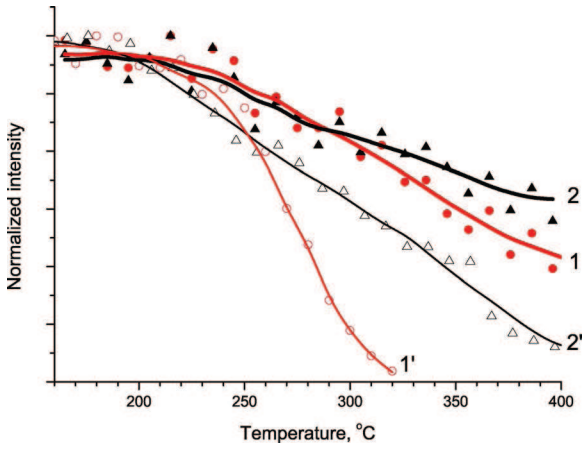

Figure 7. Temperature dependence of the intensity of the Cu-containing $[CuL_2\text{-}2OC_4H_9]^+$ and Pd-containing $[PdL]^+$ ion peaks in the mass spectra of the heterometallic complex **1** (curves 1 and 2, respectively) and the monometallic complexes CuL_2 and PdL_2 (curves 1′ and 2′, respectively).

Structural consideration

The co-crystallization of structurally related complexes CuL_2 or $Cu(tmhd)_2$ with PdL_2 yields crystals of 1D coordination polymers, as observed in the structures of **1** and **2**. Recently, we described the preparation and crystal structure of the PdL_2 complex.[6a] The structural data showed that the *trans*-PdL_2 molecules do not form coordination polymers, as observed in the structure of CuL_2. CuL_2 allows for an α-*trans* modification (3D polymer) from the solution, while sublimation results in a looser metastable β-*trans* modification with a 1D coordination polymer structure.[3e,6b] In the crystal, chains of molecules are only connected through van der Waals contacts between one another. The *tert*-butyl groups of the Pd complex are disordered due to rotation. Consequently, every strong interaction in these compounds occurs within the chains. The formation of mixed-metal coordination networks was demonstrated with other metal β-diketonate complexes, but the volatility of these networks has not been reported.[7] Based on the bond lengths in the Cu coordination site in compounds **1** and **2**, a typical redistribution of Cu–O bond lengths occurred as the coordination number increased through different degrees of interaction, which is when the chelate metal–ligand bonds are elongated due to the formation of additional coordination bonds. Specifically, the Cu–O distance in the chelate increased by 0.023 Å in **1** and by 0.015 Å in **2** relative to the length of the analogous bond in pure α-*trans*-CuL_2.[3d] Also, the C–OCH_3 bond in PdL_2 lengthens by 0.043 in **1** and by 0.035 Å in **2** relative to the bond in pure PdL_2.[6a]

Here, we can determine how the ligand structures influence the structure and properties of the corresponding heterometallic complexes. Ligands L and tmhd have similar compositions and structures. These ligands differ due to the presence of oxygen in one of the terminal substituents. Nevertheless, the bridging Cu–O bond is significantly shorter in coordination polymer **1** than in coordination polymer **2**. Because tmhd is a symmetrical ligand, phenomena such as the Jahn–Teller effect can be expected to impact the $Cu(tmhd)_2$ in structure **2**, in which the bridging Cu–O bond in the octahedral coordination site of the copper complex is longer than that in structure **1**. This difference affects the properties of these compounds (see the next section). A QTAIM analysis of the intermolecular Cu–O interactions in **1** shows that the bridging Cu–O interaction between the molecules is weak, but it binds together molecules of metal complexes to form 1D coordination polymers in the crystalline phase. The calculated mean value for length of the bridging Cu–O in trimetallic fragments (Table 1) is about 2.917 Å, which is consistent with the experimentally determined value (2.916 Å). The chain of alternating molecules in **1** seems to be an infinite superposition of the $[CuL_2{*}PdL_2{*}CuL_2]$ and $[PdL_2{*}CuL_2{*}PdL_2]$ substructures. Consequently, the calculated results agree with the structural data.

We compared the strength of the identified closed-shell interaction between the copper and oxygen atoms to classify

the intermolecular interactions in the crystals.[8a] According to this classification scheme, the strength of the Cu···O interaction is between that of strong and weak hydrogen bonds ($\rho \approx 0.08\ e\,Å^{-3}$, $G \approx 1.40\ e\,Å^{-3}$ or $19.95\ kJ\,mol^{-1}\,Bohr^{-3}$ and $U \approx -1.14\ e\,Å^{-3}$ or $-16.28\ kJ\,mol^{-1}\,Bohr^{-3}$, Table 1). Therefore, the intermolecular interactions in the chain are weak enough to hinder the transition of the heterometallic compound into the gas phase upon heating. This transition towards the dimeric fragment leads to minimal redistribution of the molecular geometry, when the bridging Cu–O bond changes slightly, and to strengthening of the intermolecular bond, based on the lowest E/ρ value (Table 1).

Magnetic properties

The magnetic properties of the heterometallic compounds were investigated based on the magnetic anisotropy predicted based on their crystal structure. We found two orthogonally related magnetic directions (Figures 4 and 5) in monocrystal **1**, which is consistent with the structural data. The observed principal values of the *A* and *g* tensors are typical for the planar environment of the copper ion.[9a] A_{zz} is parallel to g_{zz}, and their two magnetic nonequivalent directions are directed at [āb] and [ab]. In the structure of **1**, the direction of g_{zz} is perpendicular to the plane of the ligand. The EPR spectra of this compound do not reveal any dipole–dipole interactions between Cu^{II} and Pd^{II} ions, indicating that the basic state of the Pd^{II} with a $3d^8$ electronic configuration is diamagnetic. The paramagnetism of **1** is attributed to the $3d^9$ state of Cu^{II} with $S = {}^1/_2$, and the complex shape of the EPR spectra of **1** is attributed to the anisotropy of the *g* value and the HFI (hyper fine interaction) with the nuclear magnetic moment of copper. The one-dimensional spin chains show a rich range of physical phenomena based on slow relaxation effects, such as field-induced transitions, magnetic phase transitions, and soliton excitations that have been investigated through EPR.[9b–d] In our case, the combination of magnetism and volatility provides a potential route toward new thin-film materials with interesting magnetic properties.

Thermal properties

The thermal properties, including the volatility and stability, were studied using several methods. Although the volatility was not directly measured, thermogravimetric analyses and sublimation tests enabled a qualitative assessment of the volatility for comparison with a series of compounds. A single, smooth mass loss (Figure 6) is an essential criterion for a compounds exhibiting 100% volatility without decomposition. The reported heterobimetallic complexes **1** and **2**, as well as the initial monometallic Cu and Pd complexes, completely evaporate under an inert environment at atmospheric pressure, confirming their volatility. The ability of the reported heterometallic complexes to pass into the gas phase without decomposition, which generates the initial monometallic complexes, before melting was tested using vacuum sublimation in a gradient tube furnace. The volatility and thermal stability of compounds **1** and **2** depend on the structure and composition of the involved Cu^{II} complex. Heterometallic compounds sublimate at lower temperatures (ca. 140 °C for **1** and ca. 110 °C for **2**) than PdL_2 under the same vacuum conditions.[6a] The difference in the volatility was also confirmed by TGA, indicating that molecules in **2** are more weakly bound than in **1**. Consequently, most of **2** sublimated before melting. Complex **1** sublimate in one zone, even after repeated sublimation. In contrast, complex **2** sublimates in three sequential overlapping zones: $Cu(tmhd)_2$, **2**, and PdL_2, which was determined from the X-ray diffration (XRD) data and estimated based on the color change. This observation is consistent with the structural data from the investigated bimetallic compounds; **1** has the highest stability because the bonds among the constitutive molecules are the strongest. These data indicate that both complexes are volatile. However, compound **2** cannot be transported in the molecular state from the vaporization vessel to the deposition zone and for this reason it can hardly been used as an MOCVD precursor. In contrast, compound **1** is stable enough during vaporization, and will be further investigated.

The above-mentioned techniques do not allow the determination of the form in which these heterometallic complexes vaporize. To address this issue, mass spectrometric studies of the vapor-phase compositions for **1**, PdL_2, and CuL_2 were performed. In the mass spectrum of PdL_2, the molecular ion $[PdL_2]^+$ is observed, while the most intensive metal-containing peak corresponds to the fragment ion $[PdL]^+$ (Table S2). No fragments with mass higher than that of the molecular ion were recorded, indicating that PdL_2 is monomeric in the gas phase. During studies of **1**, its molecular ion $[PdL_2{*}CuL_2]^+$ was not recorded. An analysis of the mass spectra of PdL_2, CuL_2, and **1** revealed that the mass spectrum of the heterobimetallic complex contains every Pd- and Cu-containing peak present in the mass spectra of the individual monometallic complexes. No new peaks were recorded in the mass spectrum of **1**. The relative intensities of the metal-containing peaks of this material differ from those in the corresponding monometallic complexes: a different ratio of peak intensities is observed for ions containing one or two ligands. In Figure 8 the intensities of the CuL_2 and PdL_2 complexes are normalized relative to the corresponding molecular peak. For compound **1**, each Cu-containing peak is normalized to the intensity of $[CuL_2]^+$, and each Pd-containing peak is normalized to the intensity of $[PdL_2]^+$ in the same mass spectrum. Consequently, comparing the mass spectra of heterobimetallic complex **1** with those of PdL_2 and CuL_2 reveals that peaks for ions containing one ligand are two times higher in intensity than those containing two ligands. This redistribution in the peak intensities may be interpreted as follows: the monometallic moieties remain bound in the gas phase, and **1** evaporates as the heterobimetallic complex $PdL_2{*}CuL_2$, which is not stable under the ionization conditions and therefore provides monometallic ions $[CuL_2]^+$, $[PdL_2]^+$, $[CuL]^+$, $[PdL]^+$ etc.

To confirm the above assumption and to determine the conditions for depositing the metal alloy films, we investigated the thermal stability of the vaporized compounds **1**, CuL_2, and PdL_2 by mass spectrometry. An analysis of the relationship be-

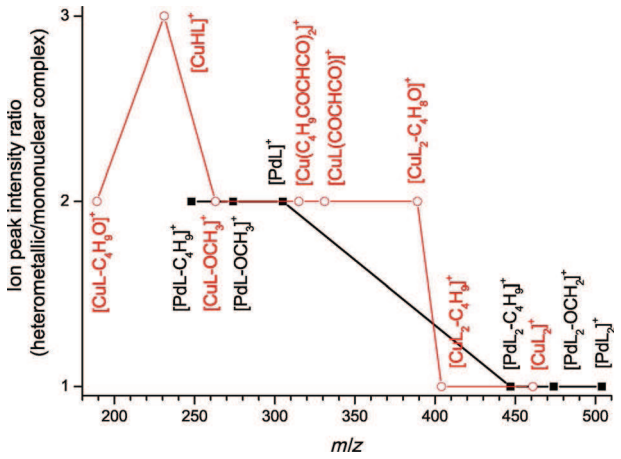

Figure 8. Ratio of the intensities of metal-containing peaks in the mass spectrum of **1** relative to that in the mass spectra of PdL_2 (black) and CuL_2 (red).

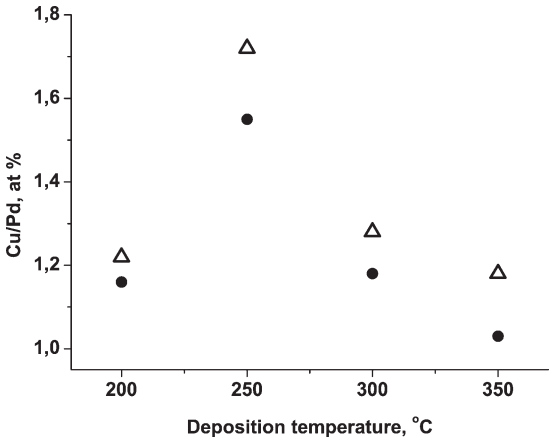

Figure 9. Cu/Pd atom ratio in the films obtained from **1** as a function of deposition temperature; circles: determined by EDS, triangles: determined by ICP-AES.

tween the temperature and the intensity of the Cu- and Pd-containing peaks obtained while subjecting the compound vapor to a heating program reveals that the Cu- and Pd-containing ion peaks for **1** match up to at least 300 °C, while these peaks differ considerably from those of the individual monometallic complexes (normalized intensity is given in Figure 7). Therefore, **1** passes into the gas phase as an individual heterobimetallic complex. In the presence of hydrogen, the thermal stability of vaporized **1** is significantly lower, and the temperature dependence of ion peaks obtained from the parent compound decline more rapidly than in vacuum (Figure S3).

Correlation with the characteristics of deposited Cu–Pd films

MOCVD of Cu–Pd-containing films was performed using **1** as a single-source molecular precursor in the presence of hydrogen. The mass spectrometry data made it possible to frame the deposition temperature in the range 200–350 °C. The detailed process parameters and characteristics of the films are presented in Ref. [5]. It is shown that films are systematically Cu-rich, with a mean Cu/Pd ratio at $T_d = 200$ °C equal to 1.2 to 1.7 depending on the technique. An increase of the Cu/Pd ratio to a mean value of 1.6 to 2.4 is observed at $T_d = 250$ °C before a decrease at about 1.2 at 350 °C. Based on data obtained in this work, we suggest the following mechanism of film growth that explains the dependence of the Cu–Pd films composition on deposition temperature. Figure 9 presents the Cu/Pd atomic ratio in the films as a function of deposition temperature. Within the temperature range of 200–250 °C interactions of the vaporized binuclear precursor CuL_2*PdL_2 with the heated substrate include thermolysis of the adsorbed compound, its dissociation into monometallic complexes, and desorption of the formed complexes. For temperatures above 250 °C dissociation becomes a predominant process and formed monometallic complexes decompose according to their proper characteristics at higher temperatures (Figure 7). This plot also reveals that the thermal stability of gaseous CuL_2 is lower than that of PdL_2; this result is compatible with the higher copper content of the films. At higher temperatures the Cu/Pd ratio in the film tends asymptotically to 1:1. Therefore, the composition of bimetallic film can be varied simply by changing the temperature of the substrate; and the optimal composition for the membrane material ($Cu_{53}Pd_{47}$)[4] can be reached at $T_d \geq 350$ °C.

Conclusion

[PdL_2*CuL_2] (**1**) and [PdL_2*$Cu(tmhd)_2$] (**2**) (L = 2-methoxy-2,6,6-trimethylheptane-3,5-dionate; tmhd = 2,2,6,6- tetramethylheptane-3,5-dionate) are a new type of molecular compounds with specific intermolecular interactions which can be utilized as a tool in the crystal engineering of volatile heterometallic complexes. The steric and electronic factors of the chelate ligands determine the crystal structure and the strength of the intermolecular interactions in these heterometallic complexes, generating materials that can sublimate to varying degrees while retaining their suprastructure. When these compounds have a particular crystal structure, they can be used for the deposition of new magnetically ordered materials. Our simultaneous consideration of complex experimental data allowed us to understand the features of the thermal behavior of these new compounds in the gas phase. Compound **1** proved to be useful as a single-source precursor for the MOCVD of Cu–Pd alloy films with a tunable Cu/Pd ratio in the range of ca. 1.6–1.0, which is promising for applications in the field of membrane materials for hydrogen separation.

Experimental Section

Synthesis and physical measurements

The preparation and identification of monometallic bis-2-methoxy-2,6,6-trimethylheptane-3,5-dionate with palladium(II) (PdL_2) and copper(II) (CuL_2) have been described in Refs. [6a] and [6b], respectively. These compounds were purified through sublimation prior to use. Heterometallic complexes were obtained after dissolving

equimolar amounts of the monometallic complexes simultaneously in a toluene/heptane mixture (1:1 v/v). Slow vaporization of the solvent under dry nitrogen flow yielded gray-green crystals for complexes **1** and **2**. These compounds were sublimated under vacuum ($P = 10^{-2}$ Torr) at $T = 140\,^{\circ}C$ and $110\,^{\circ}C$, respectively. The elemental microanalyses for carbon and hydrogen were performed using a Euro EA 3000 instrument. Compound **1**: calcd (%) for $C_{44}H_{76}O_{12}CuPd$: C 54.6, H 7.9; found: C 54.5, H 8.0. Compound **2**: calcd (%) for $C_{44}H_{76}O_{10}CuPd$: C 56.5, H 8.1; found: C 56.4, H 8.0.

The thermal properties of the compound in the solid phase were investigated using thermogravimetric and differential thermal analyses (TG-DTA) using a TG 209 F1 Iris (NETZSCH) thermobalance and a standard open crucible. The measurements were performed under atmospheric pressure in helium flow (30–40 mL min^{-1}) with a heating rate of $10\,^{\circ}C\,min^{-1}$ within the temperature range 50–350 °C.

The electron paramagnetic resonance (EPR) spectra of a single crystal (ca. 1 mm^3) of compound **1** were recorded on a Varian E-109 instrument in X-band at 300 K. The angular variations in the EPR spectrum were obtained using a goniometer with two plane rotations in two perpendicular planes, {c} and {āb}. The parameters of the EPR spectra were calculated using the Bruker WinEPR/Simfoniya software.

X-ray diffraction analyses

X-ray powder diffraction (XRD) measurements of the polycrystalline compounds were performed under ambient conditions using a Shimadzu XRD-7000 diffractometer ($Cu_{K\alpha}$ radiation, Ni filter, 2θ angle range from 5° to 50°, steps of 0.03° 2θ). The products were ground in the presence of Vaseline oil, and the resulting suspension was applied to the polished side of a standard quartz cuvette. A similarly prepared polycrystalline silicon sample was used as an external standard. The diffraction pattern of the compound was completely indexed using the XRD pattern of a single crystal with no extra lines, indicating that the product was a single phase. The unit cell parameters and experimental intensities used to solve the crystal structure were measured using a Bruker Apex Duo four-circle diffractometer with a two-dimensional CCD detector ($Mo_{K\alpha}$ radiation, graphite monochromator). The crystallographic data and experimental details are given in Table S1 of the Supporting Information. More accurate data collection and study of the structure were done for the more promising complex **1.**The structures were solved using direct methods and were refined using an anisotropic (isotropic for H) approximation. The positions of the hydrogen atoms were geometrically defined. Calculations were conducted in the SHELX-97 software.[10] CCDC 908766 for **1**, and CCDC 908767 for **2**, contain the supplementary crystallographic data for this paper. These data can be obtained free of charge via http://www.ccdc.cam.ac.uk/conts/retrieving.html, or from the Cambridge Crystallographic Data Centre, 12 Union Road, Cambridge CB2 1EZ, UK; Fax: (+44) 1223-336-033; or by e-mail: deposit@ccdc.cam.ac.uk.

Quantum chemistry computational details

The quantum theory of atoms in molecules (QTAIM) method was used to study intermolecular interactions.[8b] We explored three model systems: [CuL_2*PdL_2], [PdL_2*CuL_2*PdL_2], and [CuL_2*PdL_2*CuL_2]. According to QTAIM, the structure of a many-electron system is completely determined by the set of critical points of electron density ρ(r, R) (r and R are the coordinates of electrons and nuclei, respectively), which is hereafter referred to as ρ, at which the electron density gradient $\nabla\rho$ is zero. Four types of critical points are possible: *ncp* is the local maximum that corresponds to the positions of nuclei; *bcp* is the saddle bonding critical point; *rcp* is the saddle ring critical point; and *ccp* is the cage critical point or the local minimum of ρ. We considered only the *bcp* while investigating the intermolecular Cu···O interactions. The types of interatomic interactions are determined by the following properties, which are calculated at the critical points: electron density (ρ); the Laplacian of the electron density $\nabla^2\rho$; the densities G and U of the kinetic and potential energies, respectively; the total density of the energy $E = U + G$; and the ratio E/ρ. The Laplacian of the electron density ($\nabla^2\rho$) measures the covalence of the interatomic bonding for the negative values in the corresponding *bcp* point; for transition metals, however, $\nabla^2\rho$ can also be positive.[8c,d] The E/ρ ratio provides the full local energy per electron, and larger $|E/\rho|$ values indicate more covalence when E is negative. G, U, and the total energy E were calculated according to the method reported by Abramov.[8e] ρ was calculated for [CuL_2*PdL_2], [PdL_2*CuL_2*PdL_2], and [CuL_2* PdL_2*CuL_2] systems based on spin-restricted DFT calculations implemented in the ADF2013 code.[8f] We used the local density approximation within the Vosko–Wilk–Nusair parametrization (LDA)[8g] and the generalized gradient approximation (GGA) functional BP86.[8h,i] Standard Slater-type orbital basis sets with a triple-ξ quality, as well as two polarization functions, were employed for every atom (TZ2P).[8j] The systems were geometrically optimized in their ground state using the quasi-Newtonian method.[8k] The bonding energy (Σ) was calculated as the difference between the total energy of the system and the total energy of the isolated atoms.[8l]

Mass spectrometric study

A specially designed input system for investigating volatile metal-organic compounds was used.[11] This system ensures that the sampling and analysis are only performed on the vapor phase. Approximately 1–2 mg of the compound was placed in an open glass ampoule and was maintained at a constant temperature (150, 155, and 150 °C for **1**, PdL_2, and CuL_2, respectively) in the evaporator under dynamic vacuum conditions. The vaporized compound passed through a heated pipeline, where it entered the mass spectrometer ion source directly through a 0.2 mm effusive orifice. The ionization was performed by electrons with energy of about 70 eV. These experimental conditions exclude almost all ion–molecule collisions in the mass spectrometer. A time-of-flight mass spectrometer was used to analyze the gas phase. When necessary, hydrogen was added to the vaporized compounds. To investigate the thermal stability of the compound in the gas phase, a pipeline section was heated at $5\,^{\circ}C\,min^{-1}$. Mass spectra showing the composition of the gas phase were recorded every 2 min.

MOCVD experiments

Detailed process parameters and characteristics of the films are presented in reference [5]. It is recalled here that Cu–Pd films were deposited on Si (100) and fused silica 10×10 mm substrates in a cold-wall stainless-steel CVD reactor. Operating pressure was 10 Torr (1.33×10^3 Pa) and deposition temperature (T_d) was in the range 200 °C–350 °C. For each experiment, 30 mg of [PdL_2*CuL_2] was conditioned in a glass ampoule; it was sublimed at 130 °C and was transported to the deposition chamber under a flow of 30 standard cubic centimeters (sccm) of Ar. 100 sccm of H_2 was used as a co-reactant. The elemental composition of the films was

determined by two different techniques, namely energy-dispersive X-ray spectrometry (EDS) and inductively coupled plasma atomic emission spectroscopy (ICP-AES).[5]

Keywords: chemical vapor deposition · copper · heterometallic complexes · magnetic anisotropy · palladium

[1] a) Themed issue: Hybrid materials, *Chem. Soc. Rev.* **2011**, *40*, 453 – 1152; b) Themed Issue: Self-assembly in Inorganic Chemistry, *Dalton Trans.* **2011**, *40*, 11985 – 12396; c) Themed Issue: Metal-Organic Frameworks, *Chem. Rev.* **2012**, *112*, 673 – 1268; d) Themed Issue: Metal Organic Frameworks, *Chem. Soc. Rev.* **2014**, *43*, 1201 – 1508; e) M. Tsaroucha, Y. Aksu, J.-D. Epping, M. Driess, *ChemPlusChem* **2013**, *78*, 62 – 69; f) Themed Issue: Molecule-based Magnets, *Chem. Soc. Rev.* **2011**, *40*, 3053 – 3368; g) J. A. Mata, F. Ekkehardt Hahn, E. Peris, *Chem. Sci.* **2014**, *5*, 1723 – 1732; h) S. Shinoda, A. Mizote, M. E. Masaki, M. Yoneda, H. Miyake, H. Tsukube, *Inorg. Chem.* **2011**, *50*, 5876 – 5878; i) F. Kennedy, N. M. Shavaleev, T. Koullourou, Z. R. Bell, J. C. Jeffery, S. Faulkner, M. D. Ward, *Dalton Trans.* **2007**, 1492 – 1499; j) V. N. Kozhevnikov, M. C. Durrant, J. A. Gareth Williams, *Inorg. Chem.* **2011**, *50*, 6304 – 6313; k) T. D. Pasatoiu, J.-P. Sutter, A. M. Madalan, F. Z. Chiboub Fellah, C. Duhayon, M. Andruh, *Inorg. Chem.* **2011**, *50*, 5890 – 5898; l) J. W. Sharples, D. Collison, *Coord. Chem. Rev.* **2014**, *260*, 1 – 20.

[2] a) Ł. John, P. Sobota, *Acc. Chem. Res.* **2014**, *47*, 470; b) N. P. Kuzmina, I. P. Malkerova, A. S. Alikhanyan, A. N. Gleizes, *J. Alloys Compd.* **2004**, *374*, 315 – 319; c) A. Navulla, L. Huynh, Z. Wei, A. S. Filatov, E. V. Dikarev, *J. Am. Chem. Soc.* **2012**, *134*, 5762 – 5765; d) J. Thurston, D. Trahan, T. Ould-Ely, K. Whitmire, *Inorg. Chem.* **2004**, *43*, 3299 – 3305; e) L. G. Hubert-Pfalzgraff, *Inorg. Chem. Commun.* **2003**, *6*, 102 – 120; f) M. Veith, *J. Chem. Soc. Dalton Trans.* **2002**, 2405 – 2412; g) C. E. Knapp, J. A. Manzi, A. Kafizas, I. P. Parkin, C. J. Carmalt, *ChemPlusChem* **2014**, *79*, 1024 – 1029; h) K. L. Choy, *Prog. Mater. Sci.* **2003**, *48*, 57 – 170; i) see for example: L. Brissonneau, C. Vahlas, *Annales de Chimie-Science des Materiaux* **2000**, *25*, 81 – 90; j) A. Drozdov, S. Troyanov, in Proceedings of the 14 International Conference on chemical vapor deposition and EUROCVD-11, Eds.: M. Allendorf, C. Bernard. PV *97 – 25*, The Electrochemical Soc. Inc. Pennington, NJ, **1997**, pp 852 – 856; k) A. N. Gleizes, *Chem. Vap. Deposition* **2000**, *6*, 155 – 173.

[3] a) V. Krisyuk, I. Baidina, T. Basova, L. Bulusheva, I. Igumenov, *Eur. J. Inorg. Chem.* **2013**, 5738 – 5745; b) I. Baidina, V. Krisyuk, I. Korolkov, P. Stabnikov, *J. Struct. Chem.* **2011**, *52*, 1008; c) I. Baidina, V. Krisyuk, E. Peresypkina, P. Stabnikov, *J. Struct. Chem.* **2008**, *49*, 304 – 308; d) I. Baidina, V. Krisyuk, P. Stabnikov, *J. Struct. Chem.* **2006**, *47*, 1111 – 1116; e) S. Gromilov, I. Baidina, *J. Struct. Chem.* **2004**, *45*, 1031 – 1081.

[4] a) G. S. Burkhanov, N. B. Gorina, N. B. Kolchugina, N. R. Roshan, D. I. Slovetsky, E. M. Chistov, *Platinum Met. Rev.* **2011**, *55*, 3 – 12; b) G. Q. Lu, J. C. Diniz da Costa, M. Duke, S. Giessler, R. Socolow, R. H. Williams, T. Kreutz, *J. Colloid Interface Sci.* **2007**, *314*, 589 – 603; c) P. M. Thoen, F. Roa, J. D. Way, *Desalination* **2006**, *193*, 224 – 229; d) K. E. Coulter, J. D. Way, S. K. Gade, S. Chaudhari, D. S. Sholl, L. Semidey-Flecha, *J. Phys. Chem. C* **2010**, *114*, 17173 – 17180; e) C. Ling, L. Semidey-Flecha, D. S. Sholl, *J. Membr. Sci.* **2011**, *371*, 189 – 196; f) L. Qin, C. Jiang, *Int. J. Hydrogen Energy* **2012**, *37*, 12760 – 12764; g) S. Kajita, S. Yamaura, H. Kimura, A. Inoue, *Mater. Trans.* **2010**, *51*, 2133 – 2138; h) Y. She, S. C. Emerson, N. J. Magdefrau, S. M. Opalka, C. Thibaud-Erkey, T. H. Vanderspurt, *J. Membr. Sci.* **2014**, *452*, 203 – 211.

[5] V. V. Krisyuk, Yu. V. Shubin, F. Senocq, A. E. Turgambaeva, T. Duguet, I. K. Igumenov, C. Vahlas, *J. Cryst. Growth* **2015**, *414*, 130 – 134.

[6] a) V. Krisyuk, A. Turgambaeva, I. Igumenov, *Method of Preparation of Palladium(II) Beta-diketonate or Ketoiminate*, RU patent 2513021 C1, **2012**; b) A. P. Pisarevsky, A. I. Yanovsky, Yu. T. Struchkov, R. V. Nichiporuk, N. I. Snezhko, L. I. Martynenko, *Koord. Khim.* **1994**, *20*, 132 – 135.

[7] a) G. Aromí, P. Gamez, J. Reedijk, *Coord. Chem. Rev.* **2008**, *252*, 964 – 989; b) A. D. Burrows, M. F. Mahon, C. L. Renouf, C. Richardson, A. J. Warren, J. E. Warren, *Dalton Trans.* **2012**, *41*, 4153 – 4163; c) L. Carlucci, G. Ciani, S. Maggini, D. M. Proserpio, M. Visconti, *Chem. Eur. J.* **2010**, *16*, 12328 – 12341.

[8] a) P. Munshi, T. N. Guru Row, *CrystEngComm* **2005**, *7*, 608 – 611; b) R. F. Bader, *Atoms in Molecules: A Quantum Theory*, Clarendon, New York, **1990**; c) P. Macchi, D. M. Proserpio, A. Sironi, *J. Am. Chem. Soc.* **1998**, *120*, 13429; d) R. Bianchi, G. Gervasio, D. Marabello, *Inorg. Chem.* **2000**, *39*, 2360; e) Yu. A. Abramov, *Acta Crystallogr. Sect. A* **1997**, *53*, 264; f) Amsterdam Density Functional (ADF) Program, Release 2012.02, Vrije Universiteit: Amsterdam, Amsterdam (The Netherlands), **2012**; g) S. H. Vosko, L. Wilk, M. Nusair, *Can. J. Phys.* **1980**, *58*, 1200; h) J. P. Perdew, *Phys. Rev. B* **1986**, *33*, 8822; i) A. D. Becke, *Phys. Rev. A* **1988**, *38*, 3098; j) E. van Lenthe, E. J. Baerends, *J. Comput. Chem.* **2003**, *24*, 1142; k) L. Versluis, T. Ziegler, *J. Chem. Phys.* **1988**, *88*, 322; l) E. J. Baerends, V. Branchadell, M. Sodupe, *Chem. Phys. Lett.* **1997**, *265*, 481 – 486.

[9] a) I. N. Marov, N. A. Kostromina, *EPR and NMR in the Chemistry of Coordination Compounds (in Russian)*, Nauka, Moscow, **1979**, p. 268; b) J. van Slageren, *Top. Curr. Chem.* **2012**, *321*, 199 – 234; c) H. L. Suna, Z. M. Wang, S. Gao, *Coord. Chem. Rev.* **2010**, *254*, 1081 – 1100; d) W. X. Zhang, R. Ishikawa, B. Breedlove, M. Yamashita, *RSC Adv.* **2013**, *3*, 3772 – 3798.

[10] G. M. Sheldrick, SHELX-97, Release 97 – 1, Program for the Solution of Crystal Structures, University of Göttingen, Göttingen (Germany), **1997**.

[11] A. E. Turgambaeva, V. V. Krisyuk, P. A. Stabnikov, I. K. Igumenov, *J. Organomet. Chem.* **2007**, *692*, 5001 – 5006.